catalysts

MDPI

Article

Kinetic Model for Simultaneous Adsorption/Photodegradation Process of Alizarin Red S in Water Solution by Nano-TiO_2 under Visible Light

Rita Giovannetti *, Elena Rommozzi, Chiara Anna D'Amato and Marco Zannotti

School of Science and Technology, Chemistry Division, University of Camerino, Via S. Agostino 1, 62032 Camerino, Italy; elena.rommozzi@unicam.it (E.R.); chiaraanna.damato@unicam.it (C.A.D.); marco.zannotti@unicam.it (M.Z.)

* Correspondence: rita.giovannetti@unicam.it; Tel.: +39-0737-402-272

Academic Editors: Polycarpos Falaras, Dionysios (Dion) Demetriou Dionysiou, Giusy Lofrano, Suresh C. Pillai, Adrián M. T. Silva and Xie Quan

Received: 15 April 2016; Accepted: 1 June 2016; Published: 8 June 2016

Abstract: The simultaneous adsorption and visible light photodegradation of Alizarin Red S in water solutions were studied in real time mode by using nano-TiO_2, such as Anatase and Aeroxide P-25, supported on polypropylene strips. Kinetic results of the overall process were compared with those obtained from separated steps of adsorption and photodegradation previously studied; kinetic advantages were evidenced with the simultaneous approach. From the study of different dye concentrations, a kinetic model has been proposed which describes the overall process. This model considered two consecutive processes: The adsorption of dye on TiO_2 surface and its photodegradation. The obtained results were in good agreement with experimental data and can predict the profiles of free dye, dye adsorbed on TiO_2 and photoproduct concentrations during the total process.

Keywords: Alizarin Red S; photodegradation; visible light; titanium dioxide; kinetics

1. Introduction

Water pollution is one of the greatest problems that the world is facing today as it leads to numerous fatal diseases and it is responsible for the death of over 14,000 people every day [1]. It occurs when pollutants are discharged into water bodies without adequate treatment to remove harmful constituents. There are many sources of water pollution and several pathways through which pollutants can move [2]. Textile dyes are an important class of synthetic organic compounds which are found in water bodies coming from different sources and they represent an environmental danger [3]. In the textile industry, dyes are lost during the dyeing process; the discharge of dyes into the water is unpleasant, not only because of their color, but also because many released dyes are toxic, carcinogenic or mutagenic to life forms [4].

One of the most important families of dyes are anthraquinone dyes. Common madder (Rubia tinctorum L. Rubiaceae) produces anthraquinone dyes in its roots; one of them is Alizarin [5]. Another important example of anthraquinone derivative is Alizarin Red S (ARS), a sodium salt of Alizarin. ARS is a common water soluble anthraquinone dye extensively employed for cotton and silk manufacturing, this dye is also used in clinical practices and in geology [6]. People with skin allergies are more susceptible to its hazardous effects. Its acute toxicity leads to skin, eyes, lungs, mucous membranes and gastro-intestinal tract irritation. In chronic conditions, it leads to dermatitis [7]. Because of its synthetic origin and its complex structure of aromatic rings, ARS is difficult to remove by general chemical, physical and biological processes [8]. Wide ranges of technologies have been developed to remove this dye from wastewaters by applying catalytic and photochemical methods [9].

In recent years, the semiconductor photocatalytic process has shown great results as a low-cost, environmentally friendly and sustainable treatment technology in the removal of persistent organic compounds and microorganisms in water and wastewater [10]. Heterogeneous photocatalysis is one of the most promising technologies to remove organic pollutants from water and air [11]. TiO_2 is the most widely applied photocatalyst [12] that has been used as active in several applications such as CO_2 reduction [13,14], hydrogen production [15], air depuration [16] and wastewater treatment with total conversion of organic compounds into carbon dioxide [17–19]. The large use of TiO_2 as photocatalyst derived from its high efficiency in the decomposition of organic pollutants, its non-toxicity, biological and chemical stability, its low cost and its transparency to visible light [20].

The general mechanism of TiO_2 photocatalytic degradation of dyes by visible light (shown in Figure 1) suggests that the excitation of the adsorbed dye takes place in appropriate singlet or triplet states. The excitation of the adsorbed dye is followed by electron injection onto the conduction band of TiO_2, whereas the dye is converted into cationic dye radical that undergoes degradation to produce mineralized products as follows [21]:

$$Dye + TiO_2 \rightarrow DyeTiO_2$$

$$DyeTiO_2 + h\nu \rightarrow Dye^{\cdot +} + TiO_2\left(e^-\right)$$

$$TiO_2\left(e^-\right) + O_2 \rightarrow TiO_2 + O_2^{\cdot -}$$

$$Dye^{\cdot +} + OH^{\cdot} \rightarrow mineralized\ products$$

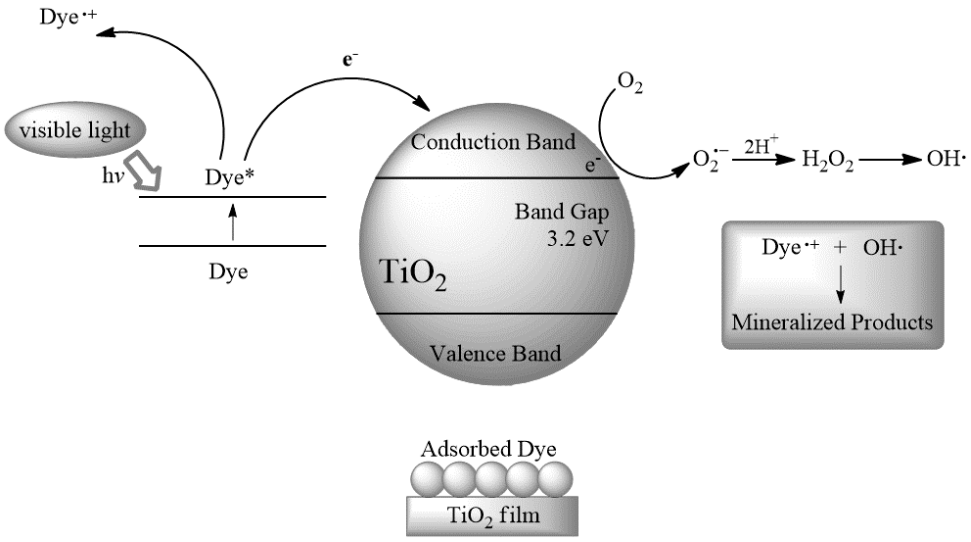

Figure 1. Mechanism of photocatalytic degradation by visible radiation.

In this study, in order to optimize and clarify the total photocatalytic mechanism of ARS as target pollutant, two commercial types of nano-TiO_2 such as Anatase and Aeroxide P-25 coated on polypropylene supports (PP@TiO_2) were used, and the simultaneous adsorption and visible light photodegradation of dye from water solution were studied. The obtained kinetic results were discussed and compared with those derived from the previous study regarding separated steps of adsorption and photodegradation [22], and a kinetic model which described the overall process in an adequate way has been proposed.

2. Results

In order to obtain a kinetic model for the total adsorption and photocatalytic degradation of ARS under visible light in water solutions, adsorption and photodegradation steps were simultaneously

studied in the same experimental conditions by changing ARS water concentrations. Figure 2 shows the change of absorbance profiles for both TiO_2 Anatase $[PP@TiO_2]_A$ (a) and TiO_2 Aeroxide P-25 $[PP@TiO_2]_{P\text{-}25}$ (b) in a typical single-step process.

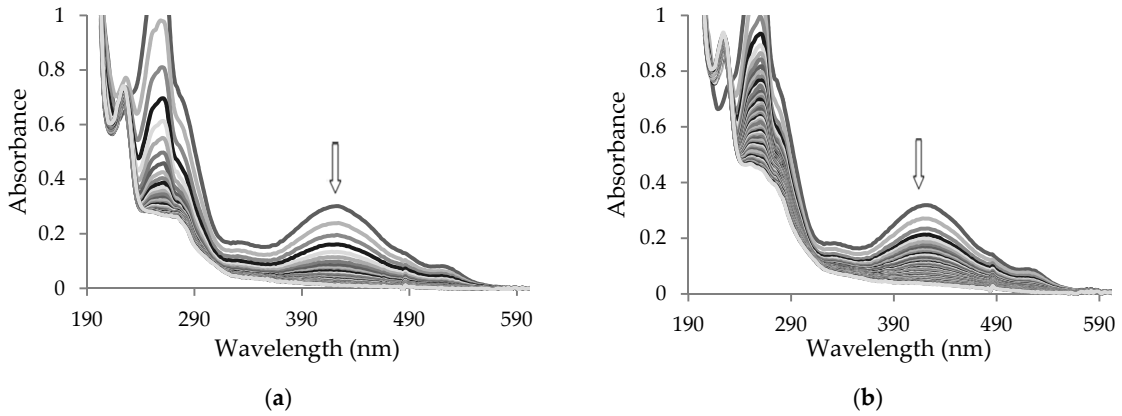

Figure 2. Decrease of UV-Vis spectra ARS solutions during the adsorption/photodegradation process under visible light by using $[PP@TiO_2]_A$ (**a**) and $[PP@TiO_2]_{P\text{-}25}$ (**b**).

The decrease of ARS solution concentrations *versus* time during the overall adsorption/photodecomposition process under visible light, for both $[PP@TiO_2]_A$ (a) and $[PP@TiO_2]_{P\text{-}25}$ (b) and for all examined ARS concentrations, is shown in Figure 3.

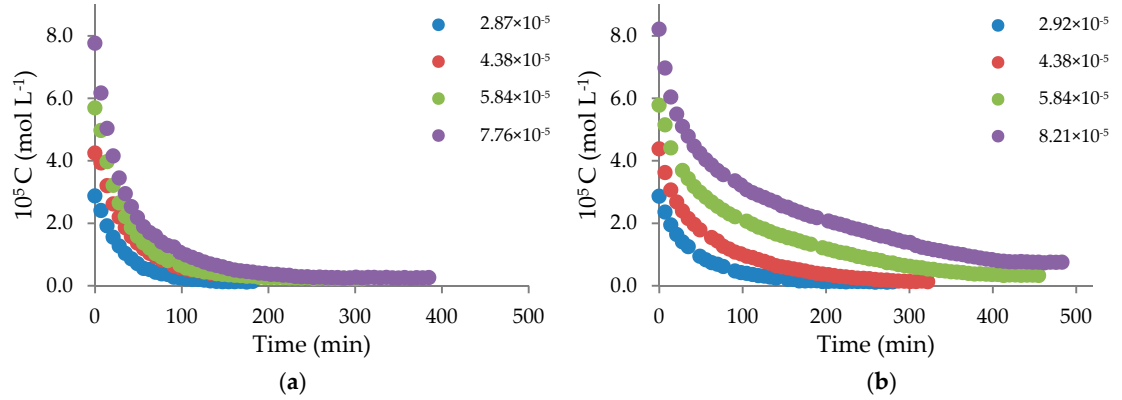

Figure 3. Decrease of ARS solution concentrations in time during the adsorption/photodegradation process under visible light by using $[PP@TiO_2]_A$ (**a**) and $[PP@TiO_2]_{P\text{-}25}$ (**b**).

However, even if the absorbance profiles during time (Figure 2) for both $[PP@TiO_2]_A$ and $[PP@TiO_2]_{P\text{-}25}$ during the process were similar, the decrease of ARS concentration during irradiation time (Figure 3), shows that the effect of initial ARS concentrations on adsorption/photodegradation rate by using $[PP@TiO_2]_A$ was different respect to that of $[PP@TiO_2]_{P\text{-}25}$. In addition, by using $[PP@TiO_2]_A$, the reaction reached completion for each initial concentration of ARS while, in the same time, by using $[PP@TiO_2]_{P\text{-}25}$ the reaction was not complete with ARS concentrations greater than 4.38×10^{-5} mol· L^{-1}.

The obtained results do not show immediate evidence in the calculation of kinetic constants because two different processes occur at the same time and correlation is never possible by using first order, second order or Langmuir-Hinshelwood kinetic models [23–26]. It is important to note that, in these simultaneous processes, obtained without a previous adsorption-desorption equilibrium in dark conditions, knowledge of the kinetic parameters of separated processes is necessary. From this consideration, the transformation of ARS to adsorbed ARS (ARS_{TiO2}) and to photodegradated

products (ARS_{PH}) could be treated in terms of two consecutive processes. The first is represented by the decrease of ARS concentration in the solution due to adsorption on PP@TiO_2 surface. The absorption of ARS is proved that occurs with a process described by the first order kinetic constant k_1 expressed by the equation $\ln[(q_e - q_t)/q_t] = -k_1 t$, where q_t is the amount of adsorbed dye at time t and q_e is the equilibrium concentration [22].

The second process is represented by photodegradation of ARS, process that occurs with a rate described by the first order kinetic constant k_2 expressed by the equation $\ln(C/C_0) = -k_2 t$ [22,23] where C_0 is the initial concentration of ARS and C the concentration of dye at t time.

$$\mathrm{ARS} + \mathrm{TiO_2} \rightarrow \mathrm{ARS_{TiO2}} \qquad k_1$$

$$\mathrm{ARS_{TiO2}} + \mathrm{h\nu} \rightarrow \mathrm{ARS}_{PH} \qquad k_2$$

The rate at which ARS decreased and the formation rates of ARS_{TiO2} and ARS_{PH} can be described as follows:

$$-\,\mathrm{d}\,[\mathrm{ARS}]/\mathrm{d}t = k_1\,[\mathrm{ARS}] \tag{1}$$

$$\mathrm{d}\,[\mathrm{ARS_{TiO2}}]/\mathrm{d}t = k_1\,[\mathrm{ARS}] - k_2\,[\mathrm{ARS_{TiO2}}] \tag{2}$$

$$\mathrm{d}\,[\mathrm{ARS}_{PH}]/dt = k_2\,[\mathrm{ARS_{TiO2}}] \tag{3}$$

The integration of Equation (1) gives:

$$[\mathrm{ARS}]_t = [\mathrm{ARS}]_0\,\mathrm{e}^{-k_1 t} \tag{4}$$

where [ARS] = $[ARS]_0$ at time 0, and [ARS] = $[ARS]_t$ at time t.

By substituting Equation (4) into Equation (2), a linear differential equation can be obtained:

$$\mathrm{d}\,[\mathrm{ARS_{TiO2}}]/\mathrm{d}t = k_1\,[\mathrm{ARS}]_0\,\mathrm{e}^{-k_1 t} - k_2\,[\mathrm{ARS_{TiO2}}] \tag{5}$$

that, after integration, can be written as:

$$[\mathrm{ARS_{TiO2}}] = \frac{k_1}{k_2 - k_1}\left(\mathrm{e}^{-k_1 t} - \mathrm{e}^{-k_2 t}\right)[\mathrm{ARS}]_0 \tag{6}$$

At any moment during the process, $[ARS]_0 = [ARS] + [ARS_{TiO2}] + [ARS_{PH}]$ so, at time t,

$$[\mathrm{ARS}_{PH}] = [\mathrm{ARS}]_0 - [\mathrm{ARS}]_t - [\mathrm{ARS_{TiO2}}]_t$$

Substituting $[ARS]_t$ and $[ARS_{TiO2}]_t$ with Equations (4) and (6) may be obtained the follow equation:

$$[\mathrm{ARS}_{PH}] = \left\{1 + \frac{k_1 e^{-k_2 t} - k_2\, e^{-k_1 t}}{k_2 - k_1}\right\}[\mathrm{ARS}]_0 \tag{7}$$

In order to prove the validity of this model it is necessary to use the values of k_1 and k_2 constants, previous described considering both the two separate processes (adsorption and photodegradation). These values are reported in Table 1.

Table 1. k_1 and k_2 for $[PP@TiO_2]_A$ and $[PP@TiO_2]_{P\text{-}25}$.

$[ARS]_0$ (mol· L^{-1})	$[PP@TiO_2]_A$ $k \times 10^2$ (min^{-1})		$[ARS]_0$ (mol· L^{-1})	$[PP@TiO_2]_{P\text{-}25}$ $k \times 10^2$ (min^{-1})	
	k_1	k_2		k_1	k_2
2.87×10^{-5}	2.57 ± 0.02	1.45 ± 0.02	2.92×10^{-5}	2.07 ± 0.02 *	1.59 ± 0.02
4.38×10^{-5}	2.54 ± 0.03	2.11 ± 0.03 *	4.38×10^{-5}	2.83 ± 0.03 *	1.55 ± 0.03 *
5.84×10^{-5}	2.27 ± 0.03	1.23 ± 0.02 *	5.84×10^{-5}	3.34 ± 0.02 *	0.67 ± 0.02 *
7.76×10^{-5}	2.62 ± 0.02	0.67 ± 0.03	8.21×10^{-5}	4.31 ± 0.04	0.34 ± 0.02

*: Reference [22].

By applying the Equation (7) obtained from the model to a simultaneous process of adsorption/photodegradation catalyzed by $[PP@TiO_2]_A$, experimental results showed a good correlation with theoretical values of $[ARS]_t$ at any time, calculated by Equation (4), by using ARS concentrations up to 5.84×10^{-5} mol· L^{-1} In Figure 4 we report, as an example, the validation model applied in the photodegradation of ARS at 5.84×10^{-5} mol· L^{-1} by $[PP@TiO_2]_A$.

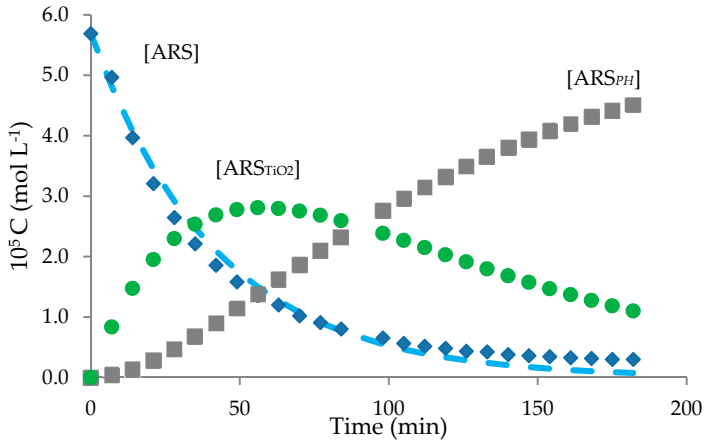

Figure 4. Changes of [ARS] (♦), [ARS_{TiO2}] (•), [ARS_{PH}] (■) and validation of model (–) *versus* time in the photodegradation of ARS at 5.84×10^{-5} mol· L^{-1} catalyzed by $[PP@TiO_2]_A$.

As it can be seen in Figure 4, while $[ARS]_t$ decreases to zero, the concentration of intermediate [ARS_{TiO2}] calculated with the Equation (6) rises to a maximum, and then falls until zero, while the concentration of [ARS_{PH}] calculated from Equation (7) rises from zero towards $[ARS]_0$. These results show that the applied model can explain the experimental data and predict the evolution of process by calculation of [ARS_{TiO_2}] and [ARS_{PH}].

When the Equation (7) of the obtained model is applied to $[PP@TiO_2]_{P\text{-}25}$, experimental results show high correlation with ARS concentrations up to 4.38×10^{-5} mol· L^{-1} as it can be seen in Figure 5, while deviations of the model occur at higher concentrations.

To explain the deviations of model for this photocatalyst it is very important to consider that, in the consecutive processes, the rate-determining step is the slowest step and it controls the overall rate of the process [27]. Therefore, in this study, the comparison of experimental results with those obtained from relative kinetic constants of two separate processes k_1 and k_2 (Table 1) it is necessary. It is possible to note that, for $[PP@TiO_2]_A$ the values of k_1 are of the same order of k_2 up to ARS concentration of 5.84×10^{-5} mol· L^{-1}, while, when k_1/k_2 ratio is greater than 2, deviations from the model occur.

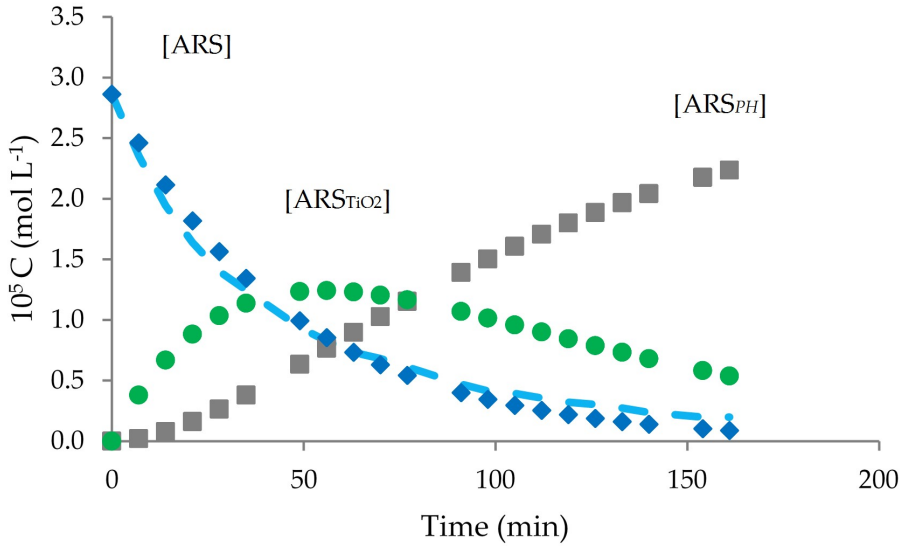

Figure 5. Changes of [ARS] (♦), [ARS_{TiO2}] (•), [ARS_{PH}] (■) and validation of model (–) *versus* time in the photodegradation of ARS at 2.92 × 10^{-5} mol· L^{-1} catalyzed by [$PP@TiO_2$]$_{P\text{-}25}$.

The same consideration applied on [$PP@TiO_2$]$_{P\text{-}25}$ gives a similar interpretation at ARS concentration up to 4.38 × 10^{-5} mol· L^{-1}, *i.e.*, the model is consistent only when k_1 and k_2 are of the same order, while deviations occur when k_1/k_2 ratio is greater than 2. Values of k_1/k_2 ratio for both [$PP@TiO_2$]$_A$ and [$PP@TiO_2$]$_{P\text{-}25}$ are reported in Table 2.

Table 2. k_1/k_2 ratio for [$PP@TiO_2$]$_A$ and [$PP@TiO_2$]$_{P\text{-}25}$.

[$PP@TiO_2$]$_A$		[$PP@TiO_2$]$_{P\text{-}25}$	
$[ARS]_0$ (mol· L^{-1})	k_1/k_2	$[ARS]_0$ (mol· L^{-1})	k_1/k_2
2.87 × 10^{-5}	1.8	2.92 × 10^{-5}	1.3
4.38 × 10^{-5}	1.2	4.38 × 10^{-5}	1.8
5.84 × 10^{-5}	1.9	5.84 × 10^{-5}	5.0
7.76 × 10^{-5}	4.0	8.21 × 10^{-5}	12.7

The slow step of these consecutive processes is therefore related to that of photodegradation process. The major influence of this, observed in the case of [$PP@TiO_2$]$_{P\text{-}25}$ and also clearly demonstrated in Figure 3b, is probably due to different adsorption behavior of [$PP@TiO_2$]$_{P\text{-}25}$ with respect to [$PP@TiO_2$]$_A$. In fact, in the case of [$PP@TiO_2$]$_{P\text{-}25}$, the absorption process is in accordance with the Langmuir model by which all dye molecules incorporated into the film have similar adsorption energy. In this case, the maximum ARS adsorption corresponds to a saturated layer of dye molecules on the TiO_2 surface that cannot contribute to an additional incorporation of other molecules. In contrast, the multilayer adsorption process according to the Freundlich isotherm occurs on [$PP@TiO_2$]$_A$ [22].

For these reasons, the absorption behavior on [$PP@TiO_2$]$_{P\text{-}25}$ at ARS concentrations over 4.38 × 10^{-5} mol· L^{-1}, mostly influences the total process because the slow photodegradation step highly limits the adsorption step. In fact, the kinetic of only monolayer absorption on this support decelerates due to a slower photodegradation process that acts as a brake in the absorption process. Moreover, to confirm this, Figure 3b shows that, for ARS concentrations over 4.38 × 10^{-5} mol· L^{-1}, two trends are present; the first is mostly related to adsorption process and correlates with k_1, while the second is related to the adsorption/photodegradation process, which is conditioned to slower kinetic constant k_2 and therefore, in this case, the rate is reduced.

The decrease of ARS solution concentration during the overall process conducted under visible light, was successive compared with those obtained from separated steps (defined with a red separation line) of adsorption in dark conditions and photodegradation under visible light, as reported in the example of Figure 6 for both $[PP@TiO_2]_A$ (a) and $[PP@TiO_2]_{P\text{-}25}$ (b).

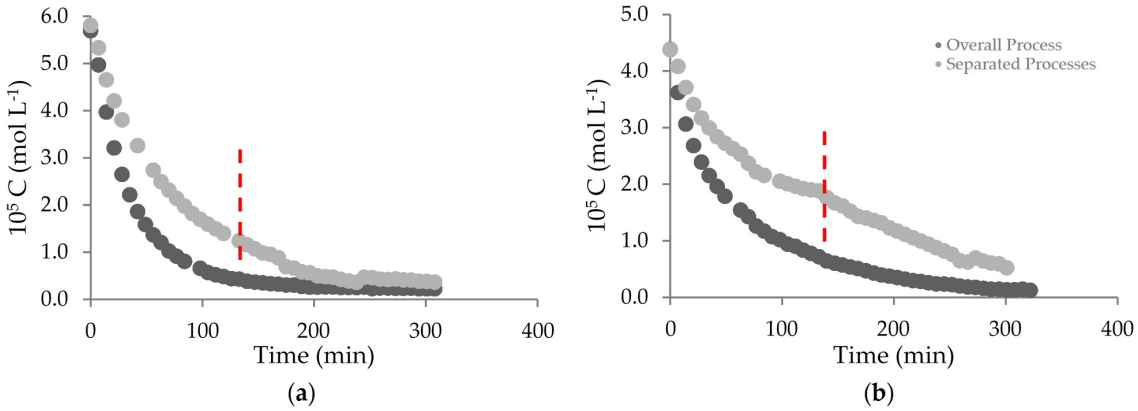

Figure 6. Comparison between ARS concentration profiles of the overall kinetic processes *versus* those obtained from separated steps for both $[PP@TiO_2]_A$ (**a**) and $[PP@TiO_2]_{P\text{-}25}$ (**b**). The red lines show the separation between adsorption and photodegradation steps.

As it may be observed in Figure 6, kinetic advantages were evidenced with the simultaneous approach showing that this method can be successfully used in water solution containing ARS.

3. Materials and Methods

3.1. Reagents and Materials

Photocatalysts were TiO_2 Anatase nano-powdered (size < 25 nm) and TiO_2 Aeroxide P-25 nano-powdered (size 21 nm), both supplied by Sigma Aldrich (Sant Louis, MO, USA). Photocatalyst support was constituted by polypropylene 2500 material obtained from 3M. Alizarin Red S, hydrochloric acid volumetric standard 1.0 N and acetyl acetone was bought from Sigma Aldrich (Sant Luis, MO, USA). Triton X-100 is purchased from Merck (Darmstadt, Hesse-Darmstadt, 64293, Germany). All of chemicals used were of analytical grade.

3.2. Methods

3.2.1. Photocatalysts Preparation

$PP@TiO_2$ photocatalysts strips were obtained as previously described in [22]. Briefly, two pastes of TiO_2 Anatase and TiO_2 Aeroxide P-25 were prepared form by a treatment with water, acetyl acetone and Triton X-100. These pastes were then supported on PP strips (of defined size with 2 cm of width and 10 cm of length) through dip coating technique, dried and clean with diluted hydrochloric acid to remove the excess of TiO_2 particles. The obtained surface was of 18 cm^2.

3.2.2. Operative Procedure for Kinetic Study

The photocatalytic activities were evaluated by ARS adsorption and photodegradation processes that were simultaneously investigated in water solutions at 25 °C and at acidic pH under the continuous action of visible light (tubular JD lamp, 80W, 1375 Lumen, Duralamp SpA, Florence, Italy) by using a glass thermostated photo reactor [22]. Nine $PP@TiO_2$ strips were immersed into ARS solutions at concentrations from 2.87×10^{-5} to 8.21×10^{-5} mol L^{-1}. Solutions were kept under constant air-equilibrated conditions before and during the irradiation. The overall process

was monitored in real-time mode every 7 min by UV-Vis spectrophotometer (Cary 8454 Diode Array System spectrophotometer, Agilent Technologies Measurements, Agilent Technologies, Santa Clara, CA, USA), using a quartz cuvette in continuous flux (Hellma Analytics, 178.710-QS, light path 10 mm, Hellma Analytics, Müllheim, Germany) connected through a peristaltic pump Gilson miniplus 3 to the photo reactor. Previously, the adsorption (in dark conditions) and photodegradation (under visible light) processes were separately investigated at the same experimental conditions [22]. All spectrophotometric measurements were performed by measuring the absorption spectra of dye solutions; the decrease in concentration of the dye, calculated at 424 nm, was plotted as function of time.

4. Conclusions

We have studied simultaneously the adsorption of ARS on [PP@TiO_2] surface and its photodegradation in order to obtain a kinetic model usefully to allow the description of the total process. Obtained results were interpreted as two consecutive reactions and were in good agreement with the experimental data.

The obtained model can predict the profiles of free dye, ARS adsorbed on TiO_2 and photoproduct concentrations during the process only when the kinetic constant that relates to adsorption process is of the same order as that of photodegradation process. In fact, when k_1/k_2 ratio is greater than 2, deviations of model are observed because the rate of the second step limits the rate of total process. These deviations are more evident in the case of [PP@TiO_2]$_{P\text{-}25}$ probably because the absorption process occurs in a monolayer form according to the Langmuir model. The absorption process, in this case, decreases for the brake due to slower photodegradation process.

Finally, when the kinetic results of the overall processes were compared with those obtained from separated steps of adsorption and photodegradation kinetic, advantages were associated with the simultaneous approach, showing that this method is appropriate in the photodegradation of water solution containing ARS, suggesting the possibility of using it with other dyes.

Author Contributions: Rita Giovannetti, Elena Rommozzi and Chiara Anna D'Amato proposed and designed the experiments; Elena Rommozzi and Chiara Anna D'Amato performed the experiments; Rita Giovannetti and Marco Zannotti analyzed the data; Rita Giovannetti contributed to reagents, materials, analysis tools; Rita Giovannetti and Elena Rommozzi wrote the paper. All the authors participated in discussions of the research.

Conflicts of Interest: The authors declare no conflict of interest.

References

1. Agrawal, A.; Pandey, R.S.; Sharma, B. Water Pollution with Special Reference to Pesticide Contamination in India. *J. Water Resource Prot.* **2010**, *2*, 432–448. [CrossRef]
2. Hill, M.K. *Understanding Environmental Pollution*, 3rd ed.; Cambridge University Press: New York, NY, USA, 2010.
3. Zaharia, C.; Suteu, D. Textile Organic Dyes—Characteristics, Polluting Effects and Separation/Elimination Procedures from Industrial Effluents—A Critical Overview. In *Organic Pollutants Ten Years after the Stockholm Convention—Environmental and Analytical Update*, 1st ed.; Puzyn, T., Ed.; InTech Europe: Rijeka, Croatia, 2012; pp. 55–86.
4. Teh, C.M.; Mohamed, A.R. Roles of titanium dioxide and ion-doped titanium dioxide on photocatalytic degradation of organic pollutants (phenolic compounds and dyes) in aqueous solutions: A review. *J. Alloys Compd.* **2011**, *509*, 1648–1660. [CrossRef]
5. Angelini, L.G.; Pistelli, L.; Belloni, P.; Bertoli, A.; Panconesi, S. *Rubia tinctorum* a source of natural dyes: Agronomic evaluation, quantitative analysis of alizarin and industrial assays. *Ind. Crop. Prod.* **1997**, *6*, 303–311. [CrossRef]
6. Dickson, J.A.D. Carbonate Identification and Genesis as Revealed by Staining. *J. Sediment. Petrol.* **1966**, *36*, 491–505.
7. Hatch, K.L.; Maibach, H.I. Textile dye dermatitis. *J. Am. Acad. Dermatol.* **1995**, *32*, 631–639. [CrossRef]

8. Gautam, R.K.; Mudhoo, A.; Chattopadhyaya, M.C. Kinetic, equilibrium, thermodynamic studies and spectroscopic analysis of Alizarin Red S removal by mustard husk. *J. Env. Chem. Eng.* **2013**, *1*, 1283–1291. [CrossRef]
9. Palmisano, G.; Augugliaro, V.; Pagliaro, M.; Palmisano, L. Photocatalysis: A promising route for 21st century organic chemistry. *Chem. Commun.* **2007**, *33*, 3425–3437. [CrossRef] [PubMed]
10. Chong, M.N.; Jin, B.; Chow, C.W.K.; Saint, C. Recent developments in photocatalytic water treatment technology: A review. *Water Res.* **2010**, *44*, 2997–3027. [CrossRef] [PubMed]
11. Kabra, K.; Chaudhary, R.; Sawhney, R. Treatment of Hazardous Organic and Inorganic Compounds through Aqueous-Phase Photocatalysis: A Review. *Ind. Eng. Chem. Res.* **2004**, *43*, 7683–7696. [CrossRef]
12. Kumar, S.G.; Devi, L.G. Review on modified TiO_2 photocatalysis under UV/visible light: Selected results and related mechanisms on interfacial charge carrier transfer dynamics. *J. Phys. Chem. A* **2011**, *115*, 13211–13241. [CrossRef] [PubMed]
13. Hamdy, M.S.; Amrollahi, R.; Sinev, I.; Mei, B.; Mul, G. Strategies to design efficient silica-supported photocatalysts for reduction of CO_2. *J. Am. Chem. Soc.* **2014**, *136*, 594–597. [CrossRef] [PubMed]
14. Tseng, I.H.; Chang, W.C.; Wu, J.C.S. Photoreduction of CO_2 using sol-gel derived titania and titania-supported copper catalysts. *Appl. Catal. B* **2002**, *37*, 37–48. [CrossRef]
15. Ni, M.; Leung, M.K.L.; Leung, D.Y.C.; Sumathy, K. A review and recent developments in photocatalytic water-splitting using TiO_2 for hydrogen production. *Renew. Sust. Energy Rev.* **2007**, *11*, 401–425. [CrossRef]
16. Mo, J.; Zhang, Y.; Xu, Q.; Lamson, J.J.; Zhao, R. Photocatalytic purification of volatile organic compounds in indoor air: A literature review. *Atmos. Environ.* **2009**, *43*, 2229–2246. [CrossRef]
17. Gaya, U.I.; Abdullah, A.H. Heterogeneous photocatalytic degradation of organic contaminants over titanium dioxide: A review of fundamentals, progress and problems. *J. Photochem. Photobiol. C* **2008**, *9*, 1–12. [CrossRef]
18. Gogate, P.R.; Pandit, A.B. A review of imperative technologies for wastewater treatment I: Oxidation technologies at ambient conditions. *Adv. Env. Res.* **2004**, *8*, 501–551. [CrossRef]
19. Fujishima, A.; Rao, T.N.; Tryk, D.A. Titanium dioxide photocatalysis. *J. Photochem. Photobiol. C* **2000**, *1*, 1–21. [CrossRef]
20. Nakata, K.; Fujishima, A. TiO_2 photocatalysis: Design and applications. *J. Photochem. Photobiol. C* **2012**, *13*, 169–189. [CrossRef]
21. Konstantinou, I.K.; Albanis, T.A. TiO_2-assisted photocatalytic degradation of azo dyes in aqueous solution: Kinetic and mechanistic investigations. A review. *Appl. Catal. B.* **2004**, *49*, 1–14. [CrossRef]
22. Giovannetti, R.; D' Amato, C.A.; Zannotti, M.; Rommozzi, E.; Gunnella, R.; Minicucci, M.; Di Cicco, A. Visible light photoactivity of Polypropylene coated Nano-TiO_2 for dyes degradation in water. *Sci. Rep.* **2015**, *5*, 17801. [CrossRef] [PubMed]
23. Chen, C.Y.; Hsu, L.J. Kinetic study of self-assembly of $Ni_{(II)}$-doped TiO_2 nanocatalysts for the photodegradation of azo pollutants. *RSC Adv.* **2015**, *5*, 88266–88271. [CrossRef]
24. Kumar, K.V.; Porkodi, K.; Selvaganapathi, A. Constrain in solving Langmuir-Hinshelwood kinetic expression for the photocatalytic degradation of Auramine O aqueous solutions by ZnO catalyst. *Dyes Pigm.* **2007**, *7*, 246–249.
25. Kesselman, J.M.; Lewis, N.S.; Hoffmann, M.R. Photoelectrochemical Degradation of 4-Chlorocatechol at TiO_2 Electrodes: Comparison between Sorption and Photoreactivity. *Environ. Sci. Technol.* **1997**, *31*, 2298–2302. [CrossRef]
26. Chen, C.Y.; Liu, Y.R. Robust and Enhanced Photocatalytic Performance of Coupled CdSe/TiO_2 Photocatalysts. *Sci. Adv. Mater.* **2015**, *7*, 1053–1057. [CrossRef]
27. Atkins, P.; De Paula, J. *Physical Chemistry*, 8th ed.; W.H. Freeman and Company: New York, NY, USA, 2006.